Zn(II) responsive MRI probe based on an Fe(III) macrocyclic complex

Roy Cineus, Aruni Dissanayake, Janet R. Morrow*

Department of Chemistry, University at Buffalo, The State University of New York
Amherst, NY 14260, United States

* to whom correspondence should be addressed at: jmorrow@buffalo.edu

Abstract

The development of responsive MRI contrast agents to detect fluctuations in Zn(II) is a growing area of research. Here we describe a high-spin Fe(III) coordination complex, Fe(ADAPT), as one of the first examples of an Fe(III) MRI probe that is responsive to Zn(II). The six-coordinate Fe(ADAPT) contains a phenolate appended 1,4,7-triazacyclononane (TACN) ligand framework with the phenolate groups linked to a Zn(II) binding moiety. Fe(ADAPT) lacks an exchangeable inner-sphere water and thus relies on second-sphere and outer-sphere water interactions for proton relaxation. Fe(ADAPT) is highly kinetically inert under physiological conditions at pH 7.4, 37 °C and to excess Zn(II) over 72 hours. In the presence of two equivalents of Zn(II) with 200 μM Fe(III) probe, an increase in relaxivity of ~80% is observed. A ternary complex between Fe(ADAPT), Zn(II), and serum albumin leads to a nearly 200% increase in relaxivity.

An important goal in biomedical research is to gain a better understanding of the role of Zn(II) homeostasis in biological processes.[1, 2] Zn(II) is tightly regulated in the human body and an imbalance may lead to adverse effects. For example, Zn(II) imbalance in the pancreas, prostate, and brain have been linked to diabetes, prostate cancer and Alzheimer's disease, respectively.[3-5] Zn(II) ions in pancreatic β cells co-release with insulin, which increases the extracellular concentration of Zn(II) to 400 – 500 μM.[6-9] The Zn(II) concentration of healthy prostate mammalian tissue is ~10 mM, but in prostate cancer tissue the Zn(II) concentration decreases ~6-fold.[3, 10, 11] Hence, monitoring Zn(II) levels may give a better understanding of these diseases towards the development of therapeutics.[12] One imaging modality for monitoring Zn(II) levels in vivo is magnetic resonance imaging (MRI). Contrast agents or probes that modulate their signal as a function of Zn(II) levels are of interest to take advantage of the high resolution and unlimited depth penetration of MRI.[1, 2]

Most Zn(II)-responsive MRI probes are based on Gd(III)[1, 2, 13] or Mn(II) complexes[14, 15] with selected probes used for in vivo experiments to monitor changes in Zn(II) levels in pancreas and in prostate.[3, 4, 14] Gd(III) complexes shorten the longitudinal relaxation (T_1) of the water protons through inner-sphere, second-sphere and outer-sphere relaxation contributions. The dipolar relaxation contribution is further governed by the number of bound water molecules (q), their exchange rate constant ($1/\tau_m$), tumbling rate constant ($1/\tau_r$), and the electronic relaxation rate constant for the paramagnetic metal ion ($1/\tau_s$).[16] For the responsive probes that are q-modulated, the Zn(II) binding moiety interacts with the Gd(III) center to block inner-sphere water in the absence of Zn(II) such as Gd(L1)[17] and Gd(L3)[18] in Scheme 1. In the presence of Zn(II), donor groups switch from Gd(III) to Zn(II) coordination, leading to an increase in q at the Gd(III) center and an corresponding increase in relaxivity ranging from 20-200%.[17-19] For the τ_r modulated complexes, Zn(II) binding results in a molecule with longer rotational times or, in some cases, an aggregate with a single Zn(II) binding to two probes.[20] Alternatively, a ternary complex with HSA may form in the presence of Zn(II), resulting in an increase in relaxivity as for Gd(L2).[6] Combining both mechanisms produces a large change in relaxivity in the presence of Zn(II). For example, binding of Zn(II) to Gd(L3) led to

dissociation of the acetate pendant to increase the q from 0 to 1 and induced formation of aggregates to increase τ_r, which led to a 400% increase in relaxivity.[18, 21]

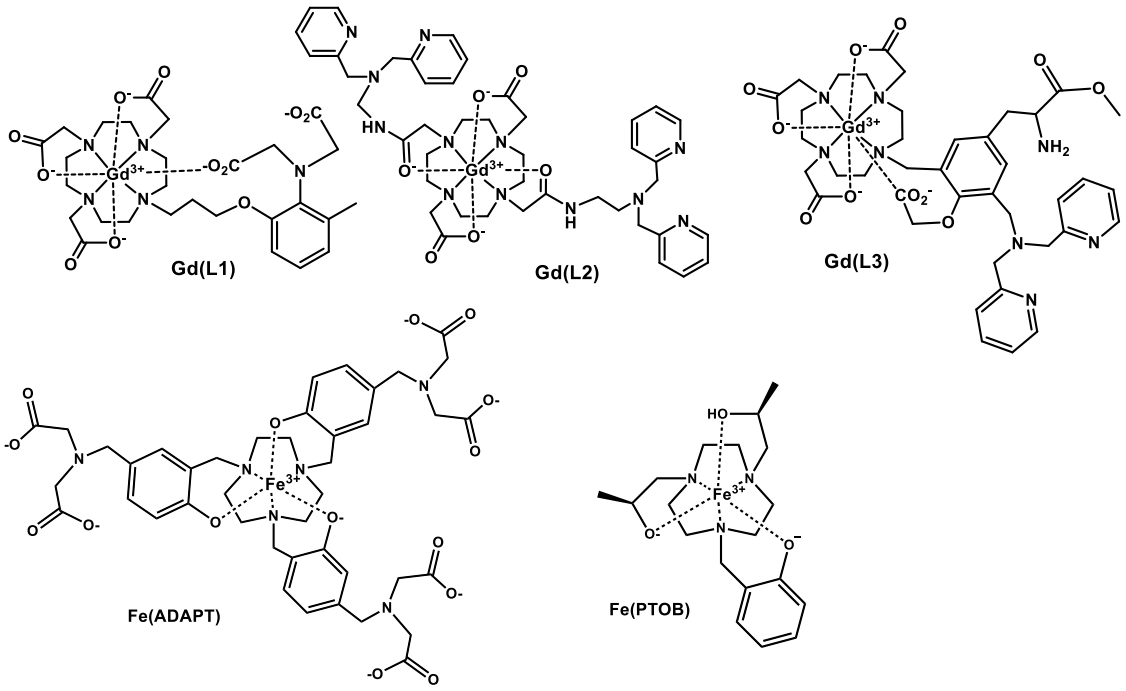

Scheme 1. MRI probes based on Gd(III) or Fe(III)

Our interest lies in developing Fe(III) based MRI contrast agents,[22, 23] to capitalize on the role of iron as an earth abundant metal ion that is stored and recycled in the human body. Here we present an Fe(III) complex that utilizes the τ_r modulated mechanism for sensing Zn(II). In these studies, the 1,4,7-triazacyclononane macrocycle (TACN) is used to capitalize on the kinetic inertness of macrocyclic complexes towards loss of iron in the presence of strong acid or to the iron transport protein, transferrin, such as observed for Fe(PTOB).[24-26] Moreover, phenolate pendants in combination with TACN macrocycles stabilize high-spin trivalent iron as shown by redox potentials of -0.80 to -1.2 V versus NHE.[27, 28] For the responsive sensor, phenol groups were functionalized with iminodiacetate to give Fe(ADAPT), which contains three binding sites for Zn(II).

The iron complex was prepared by mixing Et-ADAPT, prepared by reductive amination (Scheme S1), with ferrous chloride in methanol in the presence of ambient

oxygen. Complexation of the iron was carried out with the protected ester to avoid iron binding to the iminodiacetate (IDA) groups followed by hydrolysis of the esters to give K_6[Fe(ADAPT)]. The effective magnetic moment (μ_{eff} = 5.8) is consistent with a high spin Fe(III) complex. Solutions of Fe(ADAPT) exhibit an intense ligand to metal charge transfer (LMCT) electronic transition which is characteristic of Fe(III) with phenolate donors (Figure S5).[29-31] There were no significant changes to the LMCT band over the course of 72 hours in the presence of biologically relevant anions 0.5 mM KH_2PO_4 and 25 mM $NaHCO_3$ at pH 7.4 at 37°C or with a 20-fold excess of Zn(II) (Figures S6, S7), consistent with kinetic inertness under these conditions.

The speciation of the iron complex was studied by UV-vis spectroscopy as a function of pH (Figure S8). That there were no significant changes from pH 2-7, suggests that the phenolic oxygens remain deprotonated at acidic pH, in contrast to analogous Fe(III) phenolate complexes that have pK_a values of 1.4 to 3.5.[23, 27] The slight red shift of the LMCT band at basic pH is tentatively assigned to deprotonation of the amines of the iminodiacetate group. Further, variable temperature ^{17}O NMR studies were carried out to study water interactions (Figure S9). The ^{17}O NMR transverse relaxivity ($r_2°$) normalized to Fe(III) concentration for Fe(ADAPT) is similar to Fe(DTPA), a six-coordinate species that lacks an inner-sphere water ligand, and significantly less than Fe(CDTA), a seven-coordinate species that has a rapidly exchanging inner-sphere water.[25, 26] This suggest that Fe(ADAPT) lacks an exchangeable inner-sphere water and that second-sphere or outer-sphere interactions will drive relaxivity.[26]

Binding interactions between Fe(ADAPT) and Zn(II) were studied by isothermal titration calorimetry (ITC). Zn(II) was titrated into an aqueous solution of 0.050 mM Fe(ADAPT) to obtain a binding isotherm (Figure 1) which was fit to a sequential binding model (eq. S3). The data was best fit to n = 3 to obtain three binding constants (Table S1) of log K = 6.4 ± 0.1, 5.0 ± 0.1, and 4.0 ± 0.2 with corresponding dissociation constants (K_D) of 370 ± 20 nM, 9 ± 2 μM, and 100 ± 30 μM, respectively. These data support strong binding of the first Zn(II), 20-fold weaker binding of a second Zn(II) and even weaker binding of a third Zn(II). A reverse titration of Fe(ADAPT) into a solution of

Zn(II) was also studied (Figure S10). Under initial conditions for this titration, there is an excess of Zn(II) to the Fe(III) probe. Binding constants are given in Table S2. Interestingly, K_1 and K_2 values for the two titrations mirror each other, with K_1 representing tighter binding for titration of Zn(II) into excess probe and K_2 representing tighter binding for titration of probe into Zn(II). The similarity of K_1 for the first titration to K_2 for the reverse titration is most consistent with simple stoichiometry to produce 1:1 Zn(II) and 2:1 Zn(II)/probe complex.

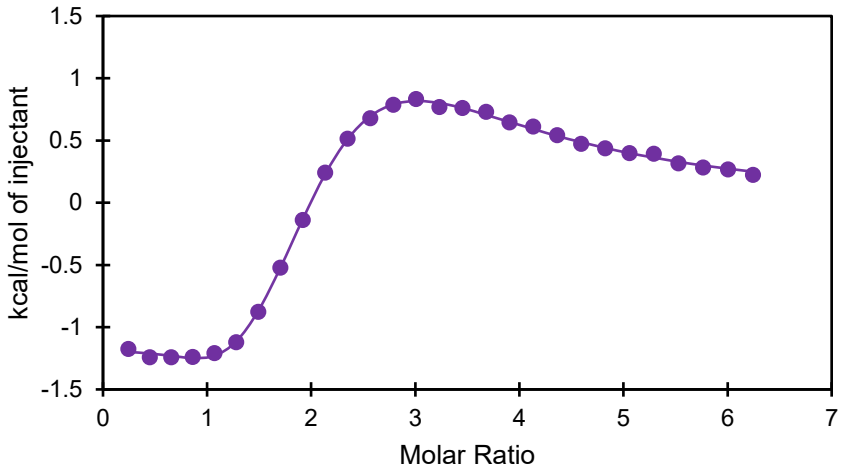

Figure 1. ITC binding isotherm of 0.050 mM Fe(ADAPT) with Zn(II) in 0.10 M NaCl, 50 mM HEPES, pH 7.4

The r_1 relaxivity of Fe(ADAPT) was studied in buffered solutions at pH 7.4 at 1.4 T (60 MHz) at 33 ºC. As shown in Figure 2A, the r_1 of Fe(ADAPT) is 1.0 $mM^{-1}s^{-1}$ in buffered solutions, consistent with an Fe(III) center lacking an exchangeable inner-sphere water.[23] There was little change in relaxivity in the presence of 0.6 mM human serum albumin (HSA) at pH 7.4, consistent with minimal binding of the probe to HSA in the absence of Zn(II). However, addition of Zn(II) increases the r_1 relaxivity of Fe(ADAPT) up to 2 equivalents of Zn(II) (~80%), followed by a slight decrease at 3 equivalents of Zn(II) (Figure 2B). We attribute the increase in relaxivity to binding of two Zn(II) ions to the Fe(ADAPT) probe to enhance second-sphere water or proton exchange as well as slower rotational correlation times. It is unlikely that Fe(ADAPT) forms multinuclear (aggregate) complexes that involve binding of one Zn(II) ion to the

IDA moieties of two different Fe(III) complexes because binding of a second IDA to Zn(II) is orders of magnitude weaker than binding of the first IDA.[32-34] Moreover, the isothermal calorimetry titrations support 1:1 or 2:1 binding of Zn(II) to probe and suggest weak binding of the third Zn(II) to the Fe(III) ADAPT probe. The slight decrease in relaxivity at > 2 ratio of Zn/probe may be related to speciation changes such as the formation of oligomeric Zn(OH) species at increasing concentrations of Zn(II).[35]

To further study the basis for the increased relaxivity of the Fe(III) complex in the presence of Zn(II), the analogous Ga(ADAPT) complex was prepared as a diamagnetic analog for NMR studies. The ^{1}H NMR spectrum of the Ga(ADAPT) complex shows nicely resolved proton resonances for the aromatic groups, the CH_2 groups of the phenolate pendants and the CH_2 of the iminodiacetates (Figure S12). Upon addition of one or two equivalents of Zn(II), the CH_2 resonances broaden, consistent with binding of Zn(II) (Figures S15 and S16). To study how binding of Zn(II) influenced the size of the probe, DOSY experiments were conducted. The diffusion coefficient initially corresponded to a hydrodynamic radius of 1.1 nm, but increased to 1.6 nm, and 1.9 nm upon addition of one or two equivalents of Zn(II) respectively (Figures S17-S19). The increase in size is consistent with binding of Zn(II) to the ADAPT probe to form larger molecules with slower rotational correlation times in solution, but does not support the formation of larger aggregates.

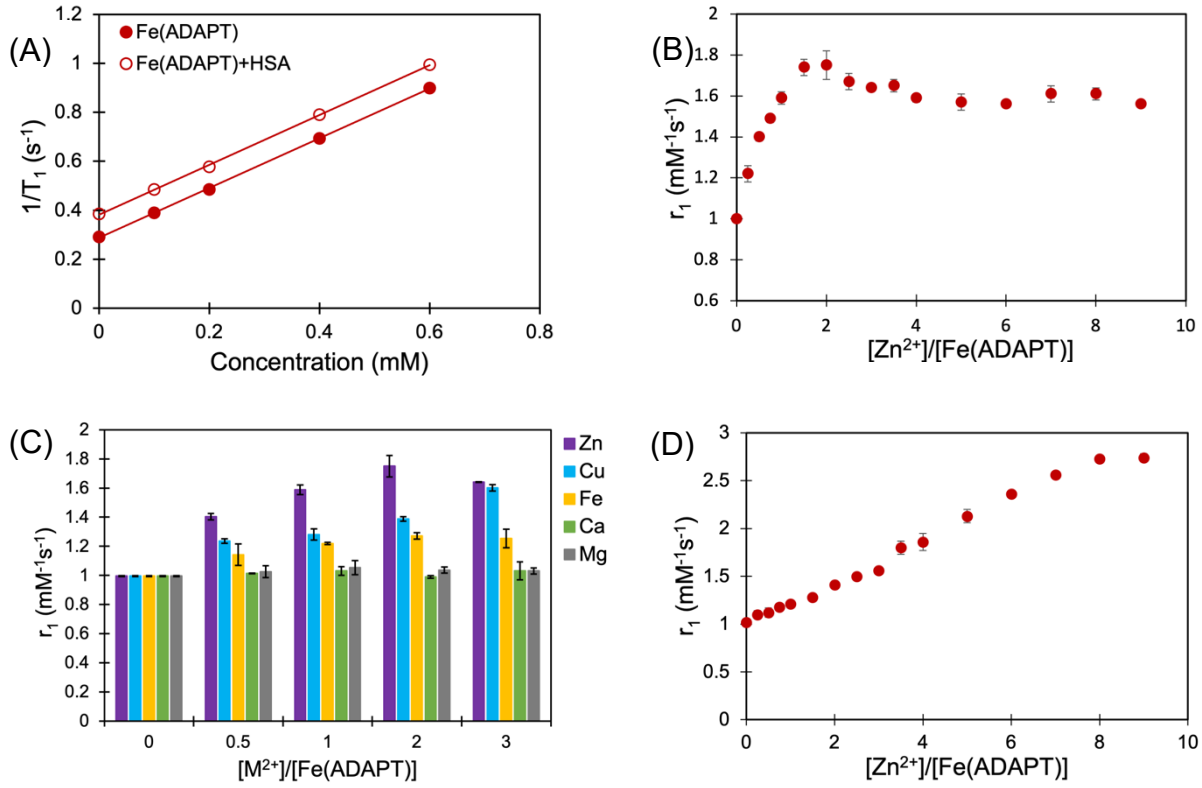

Figure 2. A) Plot of $1/T_1$ of Fe(ADAPT) as a function of probe concentration to give r_1. B) r_1 with variable Zn(II) titrated into 0.20 mM Fe(ADAPT). C) r_1 in the presence of Zn(II), Cu(II), Fe(II), Ca(II), Mg(II), with 0.20 mM Fe(ADAPT). All solutions contained 0.10 M NaCl, 50 mM HEPES, pH 7.4 and 33°C. D) Zn(II) titration of 0.20 mM Fe(ADAPT) with 0.60 mM HSA.

The selectivity of Fe(ADAPT) towards other biologically relevant metal ions was studied. No significant change in r_1 was observed for Ca(II) and Mg(II) consistent with low binding constants for the iminodiacetate moiety.[36] Moreover, the probe still responded to Zn(II) by showing an analogous increase in relaxivity in the presence of three equivalents of $CaCl_2$ (0.60 mM). Addition of Cu(II) gave an increase of ~60%, similar to that of Zn(II), whereas addition of Fe(II) produced a 20% increase at a 3:1 ratio. However, competition with these metal ions is not expected to be significant due to the low concentrations of Cu(II) and Fe(II) in blood.[37]

Studies on Zn(II) responsive contrast agents have shown that r_1 may be increased through formation of a ternary complex between the contrast agent, Zn(II), and HSA.[4, 6, 9, 38] Following this approach, Zn(II) was added to Fe(ADAPT) in the presence of 0.6 mM HSA, the concentration of HSA in vivo (Figure 2D). The r_1

increased to give a r_1 relaxivity increase of 170% at an 8:1 ratio of Zn(III) to probe. The unusual shape of the curve is postulated to arise from Zn(II) binding to HSA, then to Fe(ADAPT) along with formation of a ternary complex to HSA with correspondingly higher relaxivity (Scheme 1). This model is consistent with strong binding of Zn(II) to HSA (K_D ~30 nM).[39] Binding to HSA (0.6 mM) then to Fe(ADAPT) (0.20 mM) would require a 6:1 ratio of Zn/probe. The observed 8:1 ratio is attributed to additional weak binding to HSA.

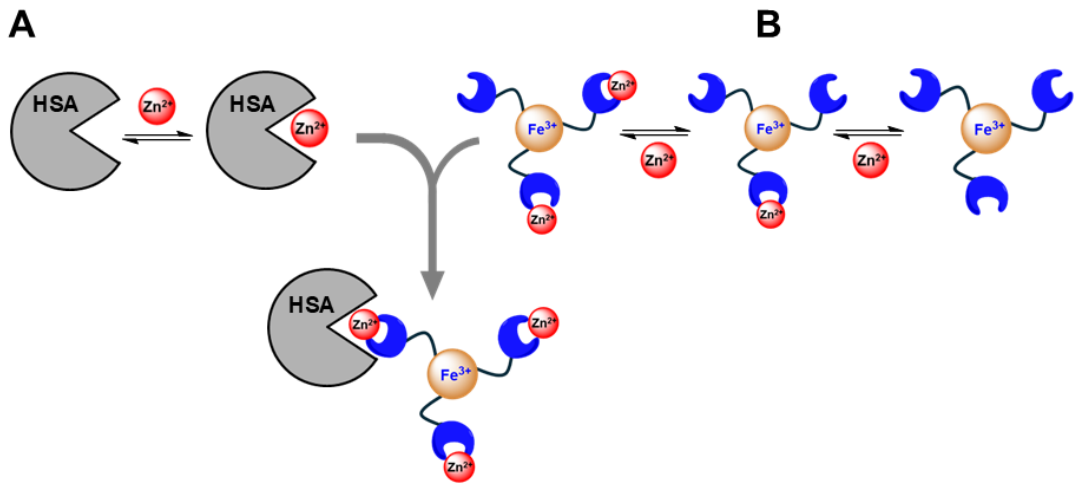

Scheme 2. Model for Zn(II) responsive probe: A) Zn(II), human serum albumin binding and B) probe and Zn(II) to give Zn-probe-HSA complex

Fe(ADAPT) represents the first Fe(III)-based MRI probe that is responsive to Zn(II), to the best of our knowledge. The probe design accommodates high-spin Fe(III) by using phenolate pendants, a TACN framework and iminodiacetates for increased water solubility of the probe and for binding of Zn(II). This framework will be used in future research by variation of Zn(II) binding moieties to better compete with HSA for Zn(II), and to modulate metal ion binding specificity as accomplished for Gd(III) probes.[2] For increased relaxivity to compete with Gd(III) probes,[2, 18] multiple Fe(III) centers may be linked in dinuclear[40] or multinuclear[41] complexes to lengthen the rotational correlation times that are limiting at moderate magnetic field strengths.[12]

Supporting Information.

Additional experimental details, materials, and methods including synthetic procedures and characterization of the ligands and Fe(III) or Ga(III) complexes by NMR spectroscopy or mass spectrometry. (DOC)

Acknowledgments.

JRM thanks the NSF (CHE-2400128) for support. We acknowledge NSF CHE-0959565 for the ICP-MS and NSF CHE-2018160 for Bruker 500 MHz NMR spectrometer.

Conflicts of Interest

JRM is cofounder of Ferric Contrast, a company that develops iron-based MRI contrast agents.

References

(1) Khalighinejad, P.; Parrott, D.; Sherry, A. D. Imaging Tissue Physiology In Vivo by Use of Metal Ion-Responsive MRI Contrast Agents. *Pharmaceuticals* **2020**, *13*, 268.

(2) Malikidogo, K. P.; Martin, H.; Bonnet, C. S. From Zn(II) to Cu(II) Detection by MRI Using Metal-Based Probes: Current Progress and Challenges. *Pharmaceuticals* **2020**, *13*, 436.

(3) Clavijo Jordan, M. V.; Lo, S.-T.; Chen, S.; Preihs, C.; Chirayil, S.; Zhang, S.; Kapur, P.; Li, W.-H.; De Leon-Rodriguez, L. M.; Lubag, A. J. M.; et al. Zinc-sensitive MRI contrast agent detects differential release of Zn(II) ions from the healthy vs. malignant mouse prostate. *Proc. Nat. Acad Sci USA* **2016**, *113*, E5464-E5471.

(4) Martins, A. F.; Clavijo Jordan, V.; Bochner, F.; Chirayil, S.; Paranawithana, N.; Zhang, S.; Lo, S.-T.; Wen, X.; Zhao, P.; Neeman, M.; et al. Imaging Insulin Secretion from Mouse Pancreas by MRI Is Improved by Use of a Zinc-Responsive MRI Sensor with Lower Affinity for Zn2+ Ions. *J Am Chem Soc* **2018**, *140*, 17456-17464.

(5) Myers, S. A.; Nield, A.; Myers, M. Zinc Transporters, Mechanisms of Action and Therapeutic Utility: Implications for Type 2 Diabetes Mellitus. *J Nutri Metab* **2012**, *2012*, 173712.

(6) Esqueda, A. C.; López, J. A.; Andreu-de-Riquer, G.; Alvarado-Monzón, J. C.; Ratnakar, J.; Lubag, A. J. M.; Sherry, A. D.; De León-Rodríguez, L. M. A New Gadolinium-Based MRI Zinc Sensor. *J Am Chem Soc* **2009**, *131*, 11387-11391.

(7) Folin, M.; Contiero, E.; Maria Vaselli, G. Zinc content of normal human serum and its correlation with some hematic parameters. *Biometals* **1994**, 75-79. .

(8) Kim, B. J.; Kim, Y. H.; Kim, S.; Kim, J. W.; Koh, J. Y.; Oh, S. H.; Lee, M. K.; Kim, K. W.; Lee, M. S. Zinc as a paracrine effector in pancreatic islet cell death. *Diabetes* **2000**, *49*, 367-372.

(9) Yu, J.; Martins, A. F.; Preihs, C.; Clavijo Jordan, V.; Chirayil, S.; Zhao, P.; Wu, Y.; Nasr, K.; Kiefer, G. E.; Sherry, A. D. Amplifying the Sensitivity of Zinc(II) Responsive MRI Contrast Agents by Altering Water Exchange Rates. *J Am Chem Soc* **2015**, *137*, 14173-14179.

(10) Costello, L. C.; Franklin, R. B. Novel role of zinc in the regulation of prostate citrate metabolism and its implications in prostate cancer. *Prostate* **1998**, 285-296.

(11) Zaichick, V.; Sviridova, T. V.; Zaichick, S. V. Zinc in the human prostate gland: normal, hyperplastic and cancerous. *Int Urol Nephrol* **1997**, *29*, 565-574.

(12) Wahsner, J.; Gale, E. M.; Rodríguez-Rodríguez, A.; Caravan, P. Chemistry of MRI Contrast Agents: Current Challenges and New Frontiers. *Chem Rev* **2019**, *119*, 957-1057.

(13) Yue, P.; Angelovski, G. How to Develop Bioresponsive MRI Probes Based on Paramagnetic Gd(III) for Applications. *Anal Sens* **2023**, *3* (6); DOI: ARTN e202300019

(14) Chirayil, S.; Jordan, V. C.; Martins, A. F.; Paranawithana, N.; Ratnakar, S. J.; Sherry, A. D. Manganese(II)-Based Responsive Contrast Agent Detects Glucose-Stimulated Zinc Secretion from the Mouse Pancreas and Prostate by MRI. *Inorg Chem* **2021**, *60*, 2168-2177.

(15) Botár, R.; Molnár, E.; Garda, Z.; Madarasi, E.; Trencsény, G.; Kiss, J.; Kálmán, F. K.; Tircsó, G. Synthesis and characterization of a stable and inert Mn^{II}-based Zn^{II} responsive MRI probe for molecular imaging of glucose stimulated zinc secretion (GSZS). *Inorg Chem Front* **2022**, *9*, 577-583.

(16) Lauffer, R. B. Paramagnetic metal complexes as water proton relaxation agents for NMR imaging: theory and design. *Chem Rev* **1987**, *87*, 901-927.

(17) Matosziuk, L. M.; Leibowitz, J. H.; Heffern, M. C.; MacRenaris, K. W.; Ratner, M. A.; Meade, T. J. Structural Optimization of Zn(II)-Activated Magnetic Resonance Imaging Probes. *Inorg Chem* **2013**, *52*,12250-12261.

(18) Wang, G.; Angelovski, G. Highly Potent MRI Contrast Agent Displaying Outstanding Sensitivity to Zinc Ions. *Angew Chem Int Ed* **2021**, *60*, 5734-5738.

(19) Major, J. L.; Boiteau, R. M.; Meade, T. J. Mechanisms of ZnII-Activated Magnetic Resonance Imaging Agents. *Inorg Chem* **2008**, *47*, 10788-10795.

(20) Malikidogo, K. P.; Isaac, M.; Uguen, A.; Morfin, J.-F.; Tircsó, G.; Tóth, É.; Bonnet, C. S. Gd3+ Complexes for MRI Detection of Zn2+ in the Presence of Human Serum Albumin: Structure–Activity Relationships. *Inorg Chem* **2023**, *62*,17207-17218.

(21) Wang, G.; Martin, H.; Amézqueta, S.; Ràfols, C.; Bonnet, C. S.; Angelovski, G. Insights into the Responding Modes of Highly Potent Gadolinium-Based Magnetic Resonance Imaging Probes Sensitive to Zinc Ions. *Inorg Chem* **2022**, *61*, 16256-16265.

(22) Kras, E. A.; Snyder, E. M.; Sokolow, G. E.; Morrow, J. R. Distinct Coordination Chemistry of Fe(III)-Based MRI Probes. *Acc Chem Res* **2022**, *55*, 1435-1444.

(23) Cineus, R.; Abozeid, S. M.; Sokolow, G. E.; Spernyak, J. A.; Morrow, J. R. Fe(III) T1 MRI Probes Containing Phenolate or Hydroxypyridine-Appended Triamine Chelates and a Coordination Site for Bound Water. *Inorg Chem* **2023**, *62*, 16513-16522.

(24) Asik, D.; Smolinski, R.; Abozeid, S. M.; Mitchell, T. B.; Turowski, S. G.; Spernyak, J. A.; Morrow, J. R. Modulating the Properties of Fe(III) Macrocyclic MRI Contrast Agents by Appending Sulfonate or Hydroxyl Groups. *Molecules* **2020**, *25*, 2291.

(25) Snyder, E. M.; Asik, D.; Abozeid, S. M.; Burgio, A.; Bateman, G.; Turowski, S. G.; Spernyak, J. A.; Morrow, J. R. A Class of FeIII Macrocyclic Complexes with Alcohol Donor Groups as Effective T1 MRI Contrast Agents. *Angew Chem Int Ed* **2020**, *59*, 2414-2419.

(26) Kras, E. A.; Abozeid, S. M.; Eduardo, W.; Spernyak, J. A.; Morrow, J. R. Comparison of phosphonate, hydroxypropyl and carboxylate pendants in Fe(III) macrocyclic complexes as MRI contrast agents. *J Inorg Biochem* **2021**, *225*, 111594.

(27) Kras, E. A.; Cineus, R.; Crawley, M. R.; Morrow, J. R. Macrocyclic complexes of Fe(III) with mixed hydroxypropyl and phenolate or amide pendants as T(1) MRI probes. *Dalton Trans* **2024**, *53*, 4154-4164.

(28) Auerbach, U.; Eckert, U.; Wieghardt, K.; Nuber, B.; Weiss, J. Synthesis and coordination chemistry of the hexadentate ligands 1,4,7-tris(2-hydroxybenzyl)-1,4,7-triazacyclononane (H3L1) and 1,4,7-tris(3-tert-butyl-2-hydroxybenzyl)-1,4,7-triazacyclononane (H3L2). Crystal structures of [HL1CuII] and [L2FeIII]acacH. *Inorg Chem* **1990**, *29*, 938-944.

(29) Auerbach, U.; Weyhermueller, T.; Wieghardt, K.; Nuber, B.; Bill, E.; Butzlaff, C.; Trautwein, A. X. First-row transition metal complexes of the hexadentate macrocycle 1,4,7-tris(5-tert-butyl-2-hydroxybenzyl)-1,4,7-triazacyclononane (LH3). Crystal structures of [LTiIV]BPh4, [LCrIII], [LFeIII], and [(LH)2FeIII2](ClO4)2.2H2O. *Inorg Chem* **1993**, *32* (5), 508-519.

(30) Adam, B.; Bill, E.; Bothe, E.; Goerdt, B.; Haselhorst, G.; Hildenbrand, K.; Sokolowski, A.; Steenken, S.; Weyhermüller, T.; Wieghardt, K. Phenoxyl Radical Complexes of Gallium, Scandium, Iron and Manganese. *Chem Eur J* **1997**, *3*, 308-319.

(31) Snodin, M. D.; Ould-Moussa, L.; Wallmann, U.; Lecomte, S.; Bachler, V.; Bill, E.; Hummel, H.; Weyhermüller, T.; Hildebrandt, P.; Wieghardt, K. The Molecular and Electronic Structure of Octahedral Tris(phenolato)iron(III) Complexes and Their Phenoxyl Radical Analogues: A Mössbauer and Resonance Raman Spectroscopic Study. *Chem Eur J* **1999**, *5*, 2554-2565.

(32) Mirti, P.; Gennaro, M. C. Nuclear magnetic resonance investigation of ligand exchange reactions in the zinc(II) ion—n-methyliminodiacetic acid system. *J Inorg Nucl Chem* **1977**, *39*, 1259-1264.

(33) Gaizer, F.; Lázár, J.; Kiss, J. T.; Póczik, E. Protonation and complex formation equilibria of N-(phenylcarbamoylmethyl)iminodiacetic acid derivatives—I. The complexes of HIDA and diethylcarbamoyl-MIDA. *Polyhedron* **1992**, *11*, 257-264.

(34) Lindblad, C.; Cassel, A.; Persson, I. Complex Formation of Alkyl-N-iminodiacetic Acids and Hard Metal Ions in Aqueous Solution and Solid State. *J Solut Chem* **2020**, *49* (9), 1250-1266.

(35) Mathews, R. A.; Rossiter, C. S.; Morrow, J. R.; Richard, J. P. A minimalist approach to understanding the efficiency of mononuclear Zn(II) complexes as catalysts of cleavage of an RNA analog. *Dalton Trans* **2007**, 3804-3811.

(36) Ando, T. Syntheses of Chelating Agents. I. Stability of the Metal Chelate of Benzylamine-N, N-diacetic Acid and its Nitro Derivatives. *Bull Chem Soc Japan* **1962**, *35*, 1395-1399.

(37) Ge, E. J.; Bush, A. I.; Casini, A.; Cobine, P. A.; Cross, J. R.; DeNicola, G. M.; Dou, Q. P.; Franz, K. J.; Gohil, V. M.; Gupta, S.; et al. Connecting copper and cancer: from transition metal signalling to metalloplasia. *Nat Rev Cancer* **2022**, *22*, 102-113.

(38) De León-Rodríguez, L. M.; Lubag, A. J. M.; López, J. A.; Andreu-de-Riquer, G.; Alvarado-Monzón, J. C.; Sherry, A. D. A second generation MRI contrast agent for imaging zinc ions in vivo. *MedChemComm* **2012**, *3*, 480-483,

(39) Masuoka, J.; Hegenauer, J.; Van Dyke, B. R.; Saltman, P. Intrinsic stoichiometric equilibrium constants for the binding of zinc(II) and copper(II) to the high affinity site of serum albumin. *J Biol Chem* **1993**, *268*, 21533-21537.

(40) Asik, D.; Abozeid, S. M.; Turowski, S. G.; Spernyak, J. A.; Morrow, J. R. Dinuclear Fe(III) Hydroxypropyl-Appended Macrocyclic Complexes as MRI Probes. *Inorg Chem* **2021**, *60*, 8651-8664.

(41) Dissanayake, A.; Spernyak, J. A.; Morrow, J. R; An octahedral coordination cage with six Fe(III) centers as a T_1 MRI probe. *Chem. Commun.* 2024, 60, 12249-12252.